

Test-Time Warmup for Multimodal Large Language Models

Nikita Rajaneesh

Columbia University

NR2937@COLUMBIA.EDU

Thomas Zollo

Columbia University

TPZ2105@COLUMBIA.EDU

Richard Zemel

Columbia University

ZEMEL@CS.COLUMBIA.EDU

Abstract

Multimodal Large Language Models (MLLMs) hold great promise for advanced reasoning at the intersection of text and images, yet they have not fully realized this potential. MLLMs typically integrate an LLM, a vision encoder, and a connector that maps the vision encoder’s embeddings into the LLM’s text embedding space. Although each component is pretrained on massive datasets with billions of samples, the entire multimodal model is typically trained on only thousands (or a few million) samples, which can result in weak performance on complex reasoning tasks. To address these shortcomings, instead of relying on extensive labeled datasets for fine-tuning, we propose a Test-Time Warmup method that adapts the MLLM per test instance by leveraging data from weakly supervised auxiliary tasks. With our approach, we observe a relative performance improvement of 4.03% on MMMU, 5.28% on VQA-Rad, and 1.63% on GQA on the Llama-Vision-Instruct model. Our method demonstrates that ‘warming up’ before inference can enhance MLLMs’ robustness across diverse reasoning tasks.

1. Introduction

In recent years, large language models (LLMs) have taken center stage in natural language processing, achieving remarkable results across a wide range of tasks (Brown et al., 2020; Minaee et al., 2025; Rae et al., 2022; Touvron et al., 2023). Concurrently, vision foundation models such as CLIP have redefined image understanding (Radford et al., 2021). Building on these advances, multimodal large language models (MLLMs) ((Grattafiori et al., 2024; Liu et al., 2023)) have shown promising performance in multimodal tasks such as image captioning (Li et al., 2023) and visual question answering (McKinzie et al., 2024), offering a vision of a future where advanced reasoning is robust across text and image.

MLLMs typically integrate an LLM, a vision encoder (e.g., CLIP), and a connector that maps the vision encoder’s embeddings into the LLM text embedding space. Despite the power of their individual components, each trained on billions of samples, for the final instruction tuning step, MLLMs are often limited by a relatively small amount of multimodal training data, typically ranging from only a few thousand to a few million examples. This lack of large-scale, end-to-end multimodal

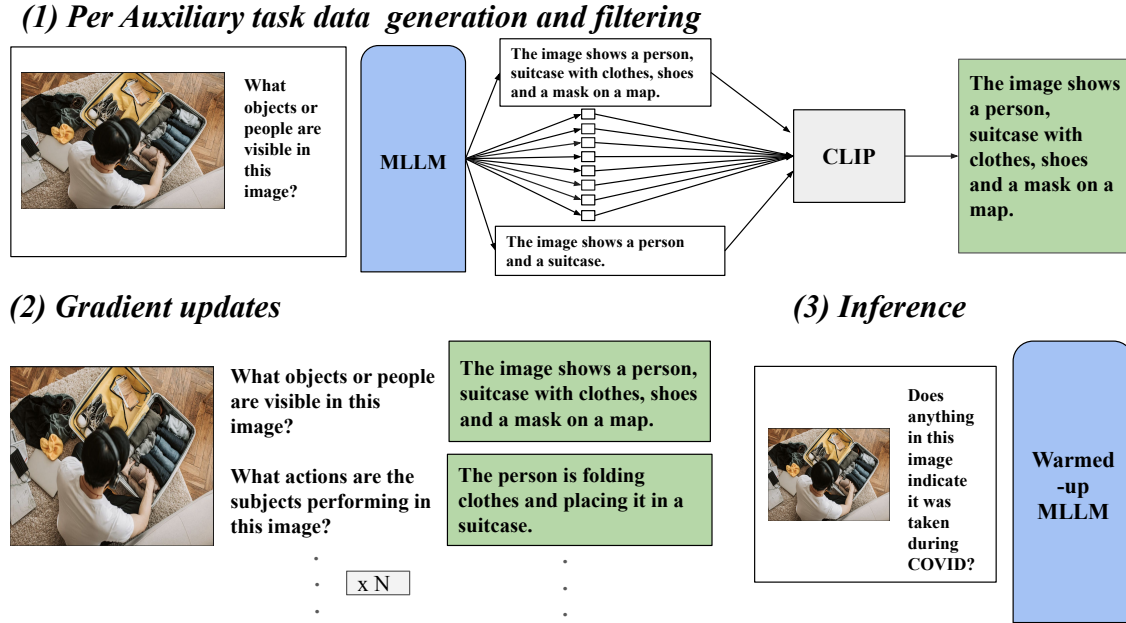


Figure 1: An example demonstrating **Test-Time Warmup** improving a model’s attention to detail (a crucial aspect of perceptual reasoning). In step (1), per auxiliary task prompt listed in Figure 2, we generate 10 caption-like outputs. In this example, we show the outputs generated for the object detection auxiliary task. Then, we use the maximum CLIP score to choose one caption. Here, the caption with more details is chosen because it’s more aligned with the image. Then in step (2), we perform gradient steps on the chosen caption-like outputs for N auxiliary task prompts ($N = 10$ as shown in Figure 2). In doing so, we enforce the model to pay attention to all the objects, including the mask, in the image. For inference, in step (3), the “warmed-up” MLLM is better informed to answer the question because it has paid attention to the mask.

supervision can hinder their ability to tackle complex reasoning tasks. Recent work has shown that MLLMs are vulnerable to distribution shifts, which undermine their reasoning capabilities (Wang et al., 2024), and they can even exhibit catastrophic forgetting and hallucinations (Zhai et al., 2023). Furthermore, research indicates that MLLMs struggle with specialized tasks, such as interpreting diagrams, due to limited task-specific training data (Joshi et al., 2025). Although fine-tuning is an effective method for addressing these challenges, the scarcity or difficulty of obtaining labeled data often makes supervised adaptation impractical in many real-world scenarios, such as medical applications.

To avoid relying on extensive labeled datasets, we introduce a novel Test-Time Warmup (TTW) method which adapts the MLLM on the fly with minimal supervision. Our method, per test instance, leverages data from weakly supervised auxiliary tasks to guide adaptation, allowing the model to refine its representations for complex reasoning without requiring any ground truth annotations. More specifically, we adapt the MLLM individually to each test instance by performing gradient updates on a set of auxiliary tasks derived from that instance. After adaptation, we perform inference on the relevant task instance and discard the updated model weights.

In this work, we focus on evaluating Test-Time Warmup and multimodal large language models (MLLMs) on visual question answering tasks using datasets such as MMMU (Yue et al., 2024), GQA (Hudson and Manning, 2019) and VQA-Rad (Narayanan et al., 2024). Through our evaluation of a popular open-source MLLM, we identify a set of failure modes indicating that these models often struggle when provided with tasks that (1) deviate substantially from the bulk of their training data, or (2) require a highly detailed understanding of the visual content.

To address these weaknesses, we propose a set of auxiliary tasks to refine image representations and “warmup” the model for inference. The auxiliary tasks are designed as input prompts to the target model and are independent of the downstream target tasks. An illustrative analogy is a “nurse practitioner and doctor” scenario: the nurse practitioner begins by asking the patient a standardized set of questions, unrelated to any specific ailment, and records the responses for the doctor. With a richer baseline of information about the patient, the doctor can then make a more accurate diagnosis.

Figure 1 provides an example of how Test-Time Warmup can prevent an MLLM from making errors. In our experiments, we find that our method outperforms baselines on datasets that focus on perceptual reasoning rather than domain knowledge. On MMMU, our approach shows gains for plot, chart or tables images: a form of data that constitutes only a small fraction of the typical training corpus and demands a deeper level of visual comprehension. In the case of GQA, which involves image-question pairs necessitating compositional reasoning, our method boosts performance for scenes that contain many subtle details. Similarly, on VQA-Rad, we see performance improvement on questions that require advanced image understanding. We attribute these gains to our method’s ability to foster more nuanced image representations and bring forth existing knowledge in the model rather than provide additional information to the model. Our main contributions include the following:

- A Test-Time Warmup method for multimodal large language models that uses data from a set of auxiliary tasks to perform gradient steps on the MLLM per test input. After adaptation, we perform inference on the test instance and discard the updated model weights.
- Using our method, we show a relative improvement of 4.03% on MMMU, 5.28% on VQA-Rad and 1.63% on GQA on Llama-Vision-Instruct model (Grattafiori et al., 2024).

Although we only show results for visual question answering tasks, through this work we motivate the use of our method to perform a diverse set of reasoning tasks. In the case of web agents, for example, performing gradient steps on a fixed set of questions and answers based on a snapshot(s) of a website (e.g., its layout, key features, or common tasks) can help orient the model to the content of that site before it attempts more specialized tasks. Overall, we offer a lightweight method, without the need for expensive labels, that has the potential to improve MLLM performance on various reasoning tasks.

2. Related work

Multimodal large language models Recently there has been a lot of interest in developing MLLMs. Well-known open-source models include Llava (Liu et al., 2023), Llama-Vision (Grattafiori et al., 2024), Qwen-VL (Bai et al., 2023b), and Gemma 3 (Team et al., 2025), and similar model

Auxiliary tasks prompts:

1. **What is happening in this image?**
2. **Describe the main subject of this image in detail.**
3. **What objects or people are visible in this image?**
4. **What actions are the subjects performing in this image?**
5. **What does the background reveal about this image?**
6. **What is unusual or unique about this image?**
7. **What details in this image might someone easily overlook?**
8. **Are there any signs, symbols or text in this image? If so, what do they say?**
9. **Explain the possible relationships or roles of the people, animals, or objects in this scene. What hints or clues suggest these relationships?**
10. **Based on visual cues, infer what might have happened just before and what might happen right after this image was captured.**

Figure 2: Each prompt represents a unique auxiliary task because the prompts are designed to elicit different kinds of information in the image from the MLLM. These auxiliary tasks are not specific to any downstream target task and they aim to refine the target image’s representations in the MLLM.

capabilities can also be found in closed-source models such as GPT-4. These models have reasonable performance on tasks similar to their training data but struggle with unseen images or tasks requiring advanced visual reasoning. For example, (Wang et al., 2024) highlight that MLLMs are susceptible to distribution shifts, which limit their multimodal reasoning. To address this, they introduce a large-scale multimodal reasoning preference dataset and propose a mixed preference optimization method to improve MLLM reasoning capabilities. This method uses a more implicit approach (preference alignment) while we focus on using auxiliary data that can directly provide context for the test example. Similarly, to improve the performance of MLLMs on specialized tasks with limited prior training, (Joshi et al., 2025) propose a method that utilizes stronger models to generate task-specific synthetic data for fine-tuning MLLMs. Instead of using stronger models, we collect auxiliary task-specific data via the same MLLM, guided by weak supervision from CLIP. This design avoids the heavy reliance on an external, more expensive labeler (human annotators or larger models) and emphasizes the use of internal resources to improve MLLM performance on specialized tasks.

Learning from Auxiliary Tasks Researchers have leveraged auxiliary tasks to boost model performance across diverse settings. Chosen as surrogates for the primary objective, these tasks steer learning toward more useful representations. In computer vision, for example, to improve object detection, Levinstein et al. (2020) train models to learn representations for semantic segmentation and distance transform. One prominent reinforcement-learning example is the UNREAL agent, which augments Atari training with unsupervised pixel-control and reward-prediction tasks that require no extra labels (Jaderberg et al., 2017). In this work, we weight all auxiliary tasks equally, whereas others, such as (Shi et al., 2020) learn task-specific importance weights. Although our

auxiliaries, like most in the literature, are manually designed, automated discovery methods are gaining traction. For instance, [Rafiee et al. \(2023\)](#) introduce an algorithm that continually generates candidate tasks and keeps those with the highest utility.

Unsupervised Domain Adaptation To avoid dependence on large labeled datasets, unsupervised domain adaptation has widely explored using auxiliary tasks across a broad range of domains and applications. For example, [Sun et al. \(2019a\)](#) leverage self-supervised auxiliary tasks to align source and target domains, improving generalization in image classification. [Zou et al. \(2018\)](#) generate pseudo-labels from target data and retrain the model to enhance performance in semantic segmentation. [Lai et al. \(2024\)](#) extend this idea to vision-language models (VLMs) by generating domain-aware pseudo-labels for visual feature refinement, enabling better adaptation of models like CLIP for unsupervised domain adaptation (UDA) in classification and detection tasks. Beyond auxiliary-task-based approaches, researchers have also explored clustering and graph-based methods for UDA ([Xiao et al., 2023](#); [Xie et al., 2018](#)). Another prominent line of work involves the use of domain adversarial loss to encourage domain-invariant feature learning and improve model generalization ([Cai et al., 2020](#); [Ganin et al., 2016](#)).

Test-Time Adaptation An increasingly popular subfield within domain adaptation is test-time adaptation (TTA), which focuses on adapting models during inference time. Test-time adaptation is particularly powerful when each test sample might come from a very different distribution, one that is difficult to handle via traditional fine-tuning. Tasks such as Abstract Reasoning Challenge ([\(Akyürek et al., 2024\)](#)) and Massive Multi-discipline Multimodal Understanding and Reasoning ([\(Yue et al., 2024\)](#)) are particularly well-suited for test-time adaptation because each test sample or a subset of samples often come from disparate distributions. Researchers first began to look at test-time training for image classification. [Sun et al. \(2019b\)](#) introduced a test-time training method that uses image rotation prediction as the auxiliary task. [Wang et al. \(2021\)](#) proposed test-time entropy minimization to reduce generalization error for image classification. [Khurana et al. \(2022\)](#) computed normalization statistics of a single unseen test-time image to perform image classification and segmentation.

Our work is also inspired by recent advances in using test-time adaptation for the Abstraction and Reasoning Challenge (ARC([Clark et al., 2018](#))). In this perceptual challenge, each example differs significantly from every other, making it difficult for traditional approaches to learn a unified representation across all possible inputs. Similarly, images (especially from different domains) can look different from each other which motivates the use of test-time adaptation to improve perceptual reasoning. [Akyürek et al. \(2024\)](#) achieve a six-fold performance improvement on ARC by applying test-time training. They enhance performance by generating auxiliary task labels and training task-specific LoRA adapters, which are discarded after inference on the target task. [Cole and Osman \(2025\)](#) similarly used test-time updates to enforce the model to perceive the ARC examples in the correct way among the the near-infinite possible image abstractions for an ARC task. They encode each ARC task (and examples) as text-sequence to train a LongT5 encoder-decoder model at test-time.

In-context Learning While test-time Training explicitly updates model parameters, In-Context Learning (ICL) instead conditions them on input at inference time without any gradient-based updates. This approach has demonstrated strong performance on a range of new tasks. For example, [Choudhary et al. \(2022\)](#) leverage auxiliary information in-context to improve short-text representations. Although

prior work (Akyürek et al., 2023) suggests that ICL might function as an implicit form of machine learning simulation, empirical results show that ICL with language models often does not align with standard machine learning algorithms (Min et al., 2022; Zhao et al., 2024). In addition, ICL can struggle with unfamiliar tasks “out-of-the-box,” as evidenced by the poor performance of large language models on datasets such as ARC (Bober-Irizar and Banerjee, 2024; Opielka et al., 2025).

3. Test-Time Warmup

In this section, we describe our algorithm for Test-Time Warmup for MLLMs. See Figure 1 for an example application of our method.

3.1. Auxiliary tasks

Ideally, generating auxiliary task information should be lightweight, requiring minimal additional computation. Beyond being cost-effective, our goal is to produce informative auxiliary data that effectively enhances multimodal reasoning capabilities.

To achieve this, we construct prompts (see Figure 2) that elicit specific types of visual information from the MLLM that might be useful context for performing more difficult tasks later. For instance, the prompt *“Are there any signs, symbols, or text in this image? If so, what do they say?”* aims to improve text recognition within images. Meanwhile, *“What objects or people are visible in this image?”* functions like an object detection task. Another example, *“Based on visual cues, infer what might have happened just before and what might happen right after this image was captured,”* encourages temporal and contextual reasoning, a valuable skill for certain types of reasoning tasks.

Each auxiliary task yields caption-like outputs. We expect these caption-like outputs to be reasonable because captioning tasks comprise a significant portion of the MLLM training mix, and thus the model may have more general abilities in captioning than other, more specialized tasks. Furthermore, CLIP models can be used to weakly supervise caption quality, as this directly aligns with their large-scale training objective.

Data generation To produce the auxiliary data for each test image, we prompt the target MLLM for 10 distinct “caption-like” responses per auxiliary task. We use vLLM for faster generation and set the temperature to 0.75 to introduce variation in the responses. This process yields a set of diverse candidate outputs for each prompt and image.

Data filtering Next, we apply a filtering step using CLIP to ensure only the most relevant and visually faithful caption is retained. Specifically, for each auxiliary task, after we generate 10 captions, we select the one with the highest CLIP score. This yields a set N captions, where N is the number of auxiliary tasks (we choose $N = 10$). This weakly supervised filtering ensures that the retained set of captions best represent the image content.

3.2. Gradient updates

Having generated and filtered the auxiliary data, we adapt the MLLM individually to each test image by performing gradient-based updates on its caption-like outputs. We freeze the vision encoder and train only the LLM and connector components using a cross-entropy loss. (We also considered other objectives, including GRPO; see *Future Work* for further discussion.) These gradient steps effectively “warmup” the model to the specific visual details of the test instance before tackling the downstream task.

3.3. Inference at test time

Once the model is adapted for a given image, we perform inference on the downstream task and then discard the updated weights. We repeat the same data generation, filtering, gradient adaptation, and inference procedure for the next test image. This per-instance adaptation strategy equips the model with a detailed understanding of each image at inference time without permanently altering the global model parameters.

4. Experiments

We conduct our experiments using the Llama-3.2-11B-Vision-Instruct model and 4 different datasets (see below for details of each). Throughout all experiments, the MLLM vision encoder remains frozen, and only the connector and LLM components are trained at test time. For each dataset, we randomly sample 500 images for our test set. We set the learning rate to 1e-6, use the AdamW optimizer [Loshchilov and Hutter \(2019\)](#), a batch size of 5, and train for 2 epochs. To ensure the model does not overfit to a specific sequence of auxiliary data, we shuffle the auxiliary examples for each image at the start of every epoch. We use CLIP-ViT to weakly supervise auxiliary data for MMMU, GQA and VQA. For VQA-Rad, which is a medical dataset, we use BiomedCLIP ([Zhang et al., 2024](#)).

4.1. Datasets

We evaluate our method on the following datasets:

MMMU ([Yue et al., 2024](#)) is designed to test multimodal understanding and reasoning capabilities at an expert level. It contains 30 subjects, including arts, science, medicine, and law, and features expert-authored multiple-choice questions that often require detailed analysis of diagrams, plots, charts, and medical images.

GQA ([Hudson and Manning, 2019](#)) is a large-scale VQA benchmark derived from Visual Genome, containing 22M questions spanning 113K images. It emphasizes compositional reasoning and scene understanding, with questions grounded in a scene graph to enable fine-grained evaluation of visual reasoning.

VQA-RAD ([Narayanan et al., 2024](#)) is a medical VQA dataset with over 3,500 clinician-authored question-answer pairs covering 315 radiology images. It focuses on clinically relevant reasoning

(e.g., identifying anatomical structures or abnormalities) and includes both open- and closed-ended questions, making it an essential benchmark for medical AI systems.

VQA (Goyal et al., 2017) is a large-scale open-ended VQA dataset consisting of 250,000 images paired with over 760,000 questions. It covers a broad range of reasoning types, such as object recognition, counting, and commonsense inference, challenging models to jointly understand vision and language.

4.2. Baselines

Base MLLM First, we consider a simple baseline. We use the huggingface open-source weights of Llama-3.2-11B-Vision-Instruct to evaluate on the sample set of 500 images for each dataset.

In-Context Learning + Our auxiliary data To demonstrate the benefits of performing test-time training on auxiliary task prompts (rather than simply providing them as in-context information for the target task), we consider the baseline where we only supply the auxiliary data (generated using the process shown in Figure 1) within the test-time prompt and without any gradient updates. The detailed prompt used for this experiment is provided in the Appendix.

4.3. Evaluation

We evaluate models using response accuracy. For GQA, VQA-Rad, and VQAv2, a response is considered correct if it contains the ground-truth answer. Additionally, for VQAv2, which includes multiple annotations, we apply the standard soft-scoring scheme that assigns higher weight to answers occurring more frequently in the annotation set. For MMMU, we report accuracy using the official evaluation code (Yue et al., 2024).¹ To ensure consistency, for a given dataset all baselines, methods, and ablations use the same evaluation strategies. The exact prompts and sampling parameters are provided in the appendix.

5. Results and Discussion

In this section, we empirically study our method’s ability to improve MLLM reasoning capabilities. We also perform ablations on the VQA-Rad dataset to understand the significance of each component in our method.

5.1. Overall performance gains from Test-Time Warmup

Our method delivers its strongest gains on benchmarks that emphasize perceptual reasoning. As Table 1 shows, Test-Time Warmup increases performance on MMMU, GQA, and VQA-Rad, all tasks that demand detailed visual understanding. In contrast, it provides only a modest improvement on VQAv2, a benchmark that leans more on general world knowledge than on perceptual cues. On

¹ We make a single change in the official code for reproducibility: for multiple-choice questions where no option can be parsed from the model’s response, we deterministically select the first option rather than a uniform random choice over the listed options.

Dataset	Base MLLM	ICL + Our auxiliary data	TTW [Ours]
GQA	61.2	62.8 (Δ 2.61%)	62.2 (Δ 1.63%)
MMMU	44.6	44.6 (Δ 0%)	46.4 (Δ 4.03%)
VQA-Rad	49.2	48.6 (Δ -1.22%)	51.8 (Δ 5.28%)
VQAv2	73.64	72.3 (Δ -1.82%)	73.84 (Δ 0.27%)

Table 1: Comparison of accuracy on Base MLLM (LLama-3.2-11B-vision-instruct), ICL (which includes auxiliary data supervised by CLIP from our method), our Test-Time Warmup method on datasets GQA, MMMU, VQA-Rad and VQAv2. In parenthesis we show the relative improvement in accuracy of Test Time Warmup compared to the base MLLM. Our model mainly shows improvement on datasets that require more advanced perceptual reasoning.

GQA, ICL+auxiliary data edges out TTW, likely because the model has already seen many natural images and can exploit in-context learning without additional gradient updates. In contrast, MMMU and VQA-Rad benefit far more from TTW, probably because the model’s pre-training included few plot-style or radiology images, making in-context learning alone insufficient.

For MMMU, GQA, and VQAv2, the reported accuracies of the base Llama-3.2-11B-Vision-Instruct model (Table 1) are obtained using basic inference techniques such as direct prompting without beam search. On MMMU, subject-specific chain-of-thought prompting for eg., can add a few percentage points. Test-Time Warmup is orthogonal to both prompting and other advanced sampling strategies and combining them can yield even greater gains. Further, although specialized medical models like LLaVA-Med achieve far higher VQA-Rad accuracies, we demonstrate that a Test-Time Warmup on a general-purpose model can still realize measurable accuracy gains by using an inexpensive medical expert such as BioMedCLIP to supervise the auxiliary data.

A key factor in attaining the results shown in Table 1 was the carefully curated set of auxiliary prompts in Figure 2, chosen to balance diversity with utility. Preliminary experiments drew ten prompts at random from a pool of fifty, but the extra variety often produced noisy, less helpful responses. We further observed that open-ended prompts (in Figure 2) were superior to constrained ones, whether limited to a specific sentence count or generated from object-detection templates (e.g., “Is object A left of object B?”). These constrained prompts offered little benefit on the higher-level reasoning tasks we target.

Figures 3, 4 and 9, 10 (in appendix) present qualitative examples from the GQA, VQA-Rad, and MMMU datasets. On MMMU, improvements were most apparent on plot- or chart-based images, which are underrepresented in typical MLLM training data and demand deeper visual comprehension. For GQA, gains were observed on examples requiring compositional reasoning and attention to subtle image details. Similarly, on VQA-Rad, the model performed better on questions involving more advanced image understanding. Across these examples, two distinct patterns emerge: (1) auxiliary task responses that explicitly surface information that directly helps answer the test question, and (2) auxiliary task responses that provide additional context or a fresh perspective on the image.

In general, we find that TTW simply “surfaces” knowledge the MLLM already holds. We sample candidate auxiliary responses, from the MLLM, at temperature 0.75 to encourage diversity, rank them with CLIP, and then take gradient steps that increases the log-likelihood of the top-ranked



Q: Are there any knives or spoons that are not large?
 Ours: no, there are no knives or spoons that are not large.
 Base MLLM: yes, there is a small spoon

Describe the main subject of this image in detail.

This image depicts a bustling food cart or food truck at night, with several people gathered around. The kitchen area is equipped with various cooking equipment, including a grill, pots, pans, and condiment bottles. **while the counter is arranged with metal pans, a bowl of ingredients, and a large pot of what appears to be potatoes.** A man on the left, wearing a white apron, holds a wrapped hot dog bun in his hand. The surrounding area is packed with people, some of whom are holding food or drinks from the cart.



Q: Are there frisbees or footballs that are not red?
 Ours: no, there are no other colors.
 Base MLLM: yes

Explain the possible relationships or roles of the people, animals or objects in this scene. What hints or clues suggest these relationships?

The image depicts a man in the midst of throwing a disc, possibly playing a game of disc golf. He is dressed in casual attire, consisting of a blue baseball cap, a blue t-shirt with a partially unbuttoned top, and plaid shorts, with his right arm extended, aiming to throw the disc. **The disc, a vibrant red, is visible in mid-air, suggesting the man's attempt to propel it forward.** The background, though blurry, appears to be a lush, grassy area surrounded by trees, with sunlight filtering through the leaves, creating a serene atmosphere. The overall scene suggests a peaceful and recreational setting.



Q: What is the piece of furniture that is behind the white bench?
 Ours: bed
 Base MLLM: headboard

Explain the possible relationships or roles of the people, animals or objects in this scene. What hints or clues suggest these relationships?

The image showcases a bed situated in a bedroom, featuring a dark brown wooden headboard or headboard-style headboard. **a white comforter and bed skirt, and a white open storage unit attached to the headboard.** Atop the headboard, a small picture frame and a row of colorful candle holders are prominently displayed. The bed is adorned with a mix of vibrant rectangular pillows in shades of red, teal, purple, and beige, adding a pop of color to the space. A red and gold tapestry hangs on the left wall, while a blue tapestry is visible on the right.

Figure 3: Examples in GQA of where our “warmed up” MLLM answers correctly while the base MLLM fails. Below each example we show the auxiliary prompt response that was the most relevant to the question and potentially aided the model for better reasoning. For the left-most image, crowded with objects and requiring fine-grained attention, the auxiliary response adds scene context that helps the model infer there are no small spoons. In the centre and right-most images, the auxiliary response explicitly provides information needed to answer the question, directly steering the model toward the correct answer.

response. This nudges the model toward information it previously under-utilized. For instance, in the far-right GQA example in Figure 3, TTW enforces the model to note the white bench—information it ignored without warmup and thus answered “headboard” incorrectly. Because CLIP can only elevate a response the model has already produced, every improvement reflects latent knowledge that TTW helps deploy.

Feeding the model a diverse set of auxiliary prompt responses improves its image-text alignment and equips it for more challenging reasoning tasks. Each auxiliary prompt encourages the model to view an image from a new angle. For instance, in the far-right VQA-Rad example in Figure 4, the auxiliary task prompt to identify anything unusual steers the model toward relevant anomalies, enabling the correct answer. By mitigating gaps in under-represented domains in MLLM training data, evidenced by our gains on MMMU and VQA-Rad, a diverse set of auxiliary data cultivates more robust image representations.

In the appendix, we also show examples of failure modes of our method.



Q: Are there rib fractures present?

Ours: no, there are no rib fractures present.
Base MLLM: yes, there are rib fractures.

What is happening in this image?

The image is a chest X-ray of a human, displaying the skeletal structure of the chest with visible bones in the rib cage, including the sternum and ribs. The lungs are also visible, although they are partially obscured by the bones.
The image is a grayscale X-ray, which allows for a clear view of the internal structures, with each bone clearly visible, indicating a normal or healthy skeletal structure. The image is titled "MedPix" in the top-right corner, and separated by a copyright symbol, indicating that it is a medical image from a medical imaging database.



Q: What kind of brain bleed is this?

Ours: subarachnoid.
Base MLLM: subdural.



Q: Is there free air under the diaphragm?

Ours: no, there is no free air under the diaphragm.
Base MLLM: yes, there is free air under the diaphragm.

What is unusual about this image?

This is one example of a chest x-ray, a medical image that provides a visual representation of the internal organs of the chest cavity, including the heart, lungs, and bones. The image appears to have a noticeable mass in the heart, which could indicate a potential health concern. The presence of this mass could suggest a variety of conditions such as a tumor, fluid accumulation, or inflammation. Further medical evaluation and diagnostic tests would be necessary to determine the cause and extent of the mass.

Figure 4: Examples in VQA-Rad of where our "warmed up" MLLM answers correctly while the base MLLM fails. Below each example we show the auxiliary prompt response that was the most relevant to the question and potentially aided the model for better reasoning. For the left-most and centre images, the auxiliary response delivers information directly needed to answer the test question. Although the auxiliary response for the far-right image is not directly tied to the question, including it in Test-Time Warmup compels the model to examine the image carefully beforehand, helping it avoid hallucinating findings that are not present.

5.2. Ablations

We perform CLIP-related ablations on the VQA-Rad dataset. We chose this dataset because we hypothesized that a medical expert, BiomedCLIP, supervising a non-medical model, Llama-3.2-11B-Vision-Instruct, would provide the most significant boost in performance.

5.2.1. AUXILIARY TASK DATA GENERATION WITHOUT SUPERVISION

To isolate the contribution of weak supervision from BiomedCLIP for VQA-Rad, we run our method without it. Specifically, we generate a single caption per prompt (instead of 10) during auxiliary data generation and perform no filtering. This ablation clarifies the performance gains attributable to BiomedCLIP-based selection of the most relevant caption-like output. As shown in Table 2, we see that BiomedCLIP supervision does improve model performance.

5.2.2. AUXILIARY TASK DATA GENERATION WITH A POOR REWARD MODEL

In the auxiliary data filtering stage, after generating 10 prompts per auxiliary task, we choose the worst generation (the lowest CLIP score we get from BiomedCLIP) to train our model on. This helps understand how a poor reward model can affect test-Time Warmup. In Table 2, we see that there’s a small difference in doing auxiliary data generation without BiomedCLIP or using the inverse of BiomedCLIP. This could possibly be due to the fact that the worst generation is bounded by the target MLLM. Additionally, the inverse of BiomedCLIP performing better than without BiomedCLIP can be due to a small amount of noise in BiomedCLIP scores.

Dataset	Base MLLM	Ours [TTW]	Ours w/o BiomedCLIP	Ours w/ Inverse of BiomedCLIP
VQA-Rad	49.2	51.8	48.8	49.6

Table 2: Comparison of accuracy of the Base MLLM (Llama-3.2-11B-Vision-Instruct) and ablations of BiomedCLIP on the VQA-Rad dataset. BiomedCLIP significantly improves accuracy on VQA-Rad.

6. Limitations and Future work

To improve the performance and efficiency of our method and to strengthen the claims we make in this work, we consider the following directions.

Models We tested our method on Qwen-VL-Chat (Bai et al., 2023a) and Gemma-12B-it (Team et al., 2025), but observed negligible improvements (less than $\Delta 0.2$ in accuracy). This highlights an important limitation, while also underscoring the need to further establish the method’s model-agnostic nature—so that, like chain-of-thought prompting, it can serve as a general framework for enhancing reasoning across diverse models.

LoRA One of the main limitations of our work is that it is computationally expensive. Instead of training the entire connector and LLM, it would be helpful to use LoRA (Hu et al., 2021) adapters. LoRA is especially helpful in settings where there is limited data. It allows efficient adaptation while maintaining the model’s general capabilities.

GRPO + online auxiliary task generation In our current approach, we use CLIP to filter auxiliary task data. Instead of filtering and discarding potentially useful information, a more effective method could be to leverage GRPO. DeepSeek-AI et al. (2025) optimize a preference using group scores of outputs generated from a single prompt. By using GRPO instead of filtering, we would avoid discarding potentially useful information. CLIP can act as the reward model. For each auxiliary task prompt, we would obtain CLIP scores for n captions and compute the GRPO loss to update the model accordingly. To obtain the most benefits from using GRPO, it could be useful to generate new responses for the auxiliary prompts after each epoch and create a self-improvement loop.

Process supervision metric We show that our method can improve the accuracy of an MLLM on benchmarks that test perceptual reasoning capabilities. To confirm that our method directly improves



Figure 5: This figure motivates using Test-Time Warmup for AI safety in MLLMs. Both the prompts shown in this figure are only offensive conditional on the image on the left because they prompt the model to make assumptions about traditional attire. For the image with children in Halloween costumes, the first question would be appropriate and for the image in the bottom right the second question would be appropriate because they are celebrating holi, a religious event.

reasoning, it would be helpful to develop a process supervision metric that measures a model’s reasoning steps before it arrives at a solution. A possible approach to do this is to use a stronger MLLM to judge the reasoning steps of the target MLLM.

Diverse set of reasoning tasks As mentioned before, we built Test-Time Warmup to adapt MLLMs for a diverse set of reasoning tasks. In this paper, we only show results for visual question answering tasks but in the future we believe an exciting direction would be to show results for web agents and other tasks that can benefit from our method.

Optimal set of auxiliary tasks We selected a small set of auxiliary task prompts that best mitigated the failure modes we observed. Future work could replace this manual selection with data-driven strategies for discovering the most effective auxiliary tasks. For example, (Ruis et al., 2025) show that, for reasoning questions, training examples rich in procedural knowledge (e.g., step-by-step formulas or code) are highly influential. A similar empirical study focused on perceptual reasoning could reveal insights to steer auxiliary-task design.

Test-Time Warmup towards AI Safety Most LLM red-teaming efforts build large, diverse prompt sets to test whether a model can refuse unsafe requests and to fine-tune its safety alignment (Perez et al., 2022; Samvelyan et al., 2024). (Zollo et al., 2024) show that such static red team datasets cannot anticipate threats that arise in complex, real-world interactions. The gap widens in multimodal

settings, where a prompt may be harmful only when paired with a specific image. Our approach provides a foundation towards safety at test-time. For each incoming image, we can first use a strong MLLM (similar to what (Perez et al., 2022) do with LLMs) to generate potential “attack prompts” (instead of using our current static set of auxiliary task prompts), then immediately adapt the target MLLM so it refuses or safely answers those prompts. Our Test-Time warmup approach can greatly expand coverage of image-conditioned threats. Figure 5 illustrates a case where a prompt is unsafe only in the presence of the accompanying image.

Acknowledgments

We thank Sruthi Sudhakar, Todd Morrill, Prof. Kaveri Thakoor, Prof. Kent Quanrud and Prof. Carl Vondrick for very helpful feedback on this work. We also thank the Google Cyber Research Program and ONR (Award N00014-23-1-2436) for their generous support. This work is supported by the funds provided by the National Science Foundation and by DoD OUSD (R&E) under Cooperative Agreement PHY-2229929 (The NSF AI Institute for Artificial and Natural Intelligence).

References

- Ekin Akyürek, Dale Schuurmans, Jacob Andreas, Tengyu Ma, and Denny Zhou. What learning algorithm is in-context learning? investigations with linear models. In *The Eleventh International Conference on Learning Representations*, 2023. URL <https://openreview.net/forum?id=0g0X4H8yN4I>.
- Ekin Akyürek, Mehul Damani, Linlu Qiu, Han Guo, Yoon Kim, and Jacob Andreas. The surprising effectiveness of test-time training for abstract reasoning, 2024. URL <https://arxiv.org/abs/2411.07279>.
- Jinze Bai, Shuai Bai, Shusheng Yang, Shijie Wang, Sinan Tan, Peng Wang, Junyang Lin, Chang Zhou, and Jingren Zhou. Qwen-vl: A versatile vision-language model for understanding, localization, text reading, and beyond, 2023a.
- Jinze Bai, Shuai Bai, Shusheng Yang, Shijie Wang, Sinan Tan, Peng Wang, Junyang Lin, Chang Zhou, and Jingren Zhou. Qwen-vl: A versatile vision-language model for understanding, localization, text reading, and beyond, 2023b. URL <https://arxiv.org/abs/2308.12966>.
- Mikel Bober-Irizar and Soumya Banerjee. Neural networks for abstraction and reasoning: Towards broad generalization in machines, 2024. URL <https://arxiv.org/abs/2402.03507>.
- Tom Brown, Benjamin Mann, Nick Ryder, Melanie Subbiah, Jared D Kaplan, Prafulla Dhariwal, Arvind Neelakantan, Pranav Shyam, Girish Sastry, Amanda Askell, Sandhini Agarwal, Ariel Herbert-Voss, Gretchen Krueger, Tom Henighan, Rewon Child, Aditya Ramesh, Daniel Ziegler, Jeffrey Wu, Clemens Winter, Chris Hesse, Mark Chen, Eric Sigler, Mateusz Litwin, Scott Gray, Benjamin Chess, Jack Clark, Christopher Berner, Sam McCandlish, Alec Radford, Ilya Sutskever, and Dario Amodei. Language models are few-shot

learners. In H. Larochelle, M. Ranzato, R. Hadsell, M.F. Balcan, and H. Lin, editors, *Advances in Neural Information Processing Systems*, volume 33, pages 1877–1901. Curran Associates, Inc., 2020. URL https://proceedings.neurips.cc/paper_files/paper/2020/file/1457c0d6bfc4967418bfb8ac142f64a-Paper.pdf.

Guanyu Cai, Yuqin Wang, Lianghua He, and MengChu Zhou. Unsupervised domain adaptation with adversarial residual transform networks. *IEEE Transactions on Neural Networks and Learning Systems*, 31(8):3073–3086, August 2020. ISSN 2162-2388. doi: 10.1109/tnnls.2019.2935384. URL <http://dx.doi.org/10.1109/TNNLS.2019.2935384>.

Nurendra Choudhary, Charu C. Aggarwal, Karthik Subbian, and Chandan K. Reddy. Self-supervised short-text modeling through auxiliary context generation. *ACM Trans. Intell. Syst. Technol.*, 13(3), April 2022. ISSN 2157-6904. doi: 10.1145/3511712. URL <https://doi.org/10.1145/3511712>.

Peter Clark, Isaac Cowhey, Oren Etzioni, Tushar Khot, Ashish Sabharwal, Carissa Schoenick, and Oyvind Tafjord. Think you have solved question answering? try arc, the ai2 reasoning challenge, 2018. URL <https://arxiv.org/abs/1803.05457>.

Jack Cole and Mohamed Osman. Don’t throw the baby out with the bathwater: How and why deep learning for arc, 2025. URL <https://arxiv.org/abs/2506.14276>.

DeepSeek-AI, Daya Guo, Dejian Yang, Haowei Zhang, Junxiao Song, Ruoyu Zhang, Runxin Xu, Qihao Zhu, Shirong Ma, Peiyi Wang, Xiao Bi, Xiaokang Zhang, Xingkai Yu, Yu Wu, Z. F. Wu, Zhibin Gou, Zhihong Shao, Zhuoshu Li, Ziyi Gao, Aixin Liu, Bing Xue, Bingxuan Wang, Bochao Wu, Bei Feng, Chengda Lu, Chenggang Zhao, Chengqi Deng, Chenyu Zhang, Chong Ruan, Damai Dai, Deli Chen, Dongjie Ji, Erhang Li, Fangyun Lin, Fucong Dai, Fuli Luo, Guangbo Hao, Guanting Chen, Guowei Li, H. Zhang, Han Bao, Hanwei Xu, Haocheng Wang, Honghui Ding, Huajian Xin, Huazuo Gao, Hui Qu, Hui Li, Jianzhong Guo, Jiashi Li, Jiawei Wang, Jingchang Chen, Jingyang Yuan, Junjie Qiu, Junlong Li, J. L. Cai, Jiaqi Ni, Jian Liang, Jin Chen, Kai Dong, Kai Hu, Kaige Gao, Kang Guan, Kexin Huang, Kuai Yu, Lean Wang, Lecong Zhang, Liang Zhao, Litong Wang, Liyue Zhang, Lei Xu, Leyi Xia, Mingchuan Zhang, Minghua Zhang, Minghui Tang, Meng Li, Miaojun Wang, Mingming Li, Ning Tian, Panpan Huang, Peng Zhang, Qiancheng Wang, Qinyu Chen, Qiushi Du, Ruiqi Ge, Ruisong Zhang, Ruizhe Pan, Runji Wang, R. J. Chen, R. L. Jin, Ruyi Chen, Shanghao Lu, Shangyan Zhou, Shanhua Chen, Shengfeng Ye, Shiyu Wang, Shuiping Yu, Shunfeng Zhou, Shuting Pan, S. S. Li, Shuang Zhou, Shaoqing Wu, Shengfeng Ye, Tao Yun, Tian Pei, Tianyu Sun, T. Wang, Wangding Zeng, Wanja Zhao, Wen Liu, Wenfeng Liang, Wenjun Gao, Wenqin Yu, Wentao Zhang, W. L. Xiao, Wei An, Xiaodong Liu, Xiaohan Wang, Xiaokang Chen, Xiaotao Nie, Xin Cheng, Xin Liu, Xin Xie, Xingchao Liu, Xinyu Yang, Xinyuan Li, Xuecheng Su, Xuheng Lin, X. Q. Li, Xiangyue Jin, Xiaojin Shen, Xiaosha Chen, Xiaowen Sun, Xiaoxiang Wang, Xinnan Song, Xinyi Zhou, Xianzu Wang, Xinxia Shan, Y. K. Li, Y. Q. Wang, Y. X. Wei, Yang Zhang, Yanhong Xu, Yao Li, Yao Zhao, Yaofeng Sun, Yaohui Wang, Yi Yu, Yichao Zhang, Yifan Shi, Yiliang Xiong, Ying He, Yishi Piao, Yisong Wang, Yixuan Tan, Yiyang Ma, Yiyuan Liu, Yongqiang Guo, Yuan Ou, Yuduan Wang, Yue Gong, Yuheng Zou, Yujia He, Yunfan Xiong, Yuxiang Luo, Yuxiang You, Yuxuan Liu, Yuyang Zhou, Y. X. Zhu, Yanhong Xu, Yanping Huang, Yaohui Li, Yi Zheng, Yuchen Zhu, Yunxian Ma, Ying Tang, Yukun Zha, Yuting Yan, Z. Z. Ren, Zehui Ren, Zhangli Sha, Zhe Fu, Zhean Xu, Zhenda Xie, Zhengyan Zhang,

Zhewen Hao, Zhicheng Ma, Zhigang Yan, Zhiyu Wu, Zihui Gu, Zijia Zhu, Zijun Liu, Zilin Li, Ziwei Xie, Ziyang Song, Zizheng Pan, Zhen Huang, Zhipeng Xu, Zhongyu Zhang, and Zhen Zhang. Deepseek-r1: Incentivizing reasoning capability in llms via reinforcement learning, 2025. URL <https://arxiv.org/abs/2501.12948>.

Yaroslav Ganin, Evgeniya Ustinova, Hana Ajakan, Pascal Germain, Hugo Larochelle, François Fleuret, Mario Marchand, and Victor Lempitsky. Domain-adversarial training of neural networks, 2016. URL <https://arxiv.org/abs/1505.07818>.

Yash Goyal, Tejas Khot, Douglas Summers-Stay, Dhruv Batra, and Devi Parikh. Making the v in vqa matter: Elevating the role of image understanding in visual question answering, 2017.

Aaron Grattafiori, Abhimanyu Dubey, Abhinav Jauhri, Abhinav Pandey, Abhishek Kadian, Ahmad Al-Dahle, Aiesha Letman, Akhil Mathur, Alan Schelten, Alex Vaughan, Amy Yang, Angela Fan, Anirudh Goyal, Anthony Hartshorn, Aobo Yang, Archi Mitra, Archie Sravankumar, Artem Korenev, Arthur Hinsvark, Arun Rao, Aston Zhang, Aurelien Rodriguez, Austen Gregerson, Ava Spataru, Baptiste Roziere, Bethany Biron, Binh Tang, Bobbie Chern, Charlotte Caucheteux, Chaya Nayak, Chloe Bi, Chris Marra, Chris McConnell, Christian Keller, Christophe Touret, Chunyang Wu, Corinne Wong, Cristian Canton Ferrer, Cyrus Nikolaidis, Damien Allonsius, Daniel Song, Danielle Pintz, Danny Livshits, Danny Wyatt, David Esiobu, Dhruv Choudhary, Dhruv Mahajan, Diego Garcia-Olano, Diego Perino, Dieuwke Hupkes, Egor Lakomkin, Ehab AlBadawy, Elina Lobanova, Emily Dinan, Eric Michael Smith, Filip Radenovic, Francisco Guzmán, Frank Zhang, Gabriel Synnaeve, Gabrielle Lee, Georgia Lewis Anderson, Govind Thattai, Graeme Nail, Gregoire Mialon, Guan Pang, Guillem Cucurell, Hailey Nguyen, Hannah Korevaar, Hu Xu, Hugo Touvron, Iliyan Zarov, Imanol Arrieta Ibarra, Isabel Kloumann, Ishan Misra, Ivan Evtimov, Jack Zhang, Jade Copet, Jaewon Lee, Jan Geffert, Jana Vranes, Jason Park, Jay Mahadeokar, Jeet Shah, Jelmer van der Linde, Jennifer Billock, Jenny Hong, Jenya Lee, Jeremy Fu, Jianfeng Chi, Jianyu Huang, Jiawen Liu, Jie Wang, Jiecao Yu, Joanna Bitton, Joe Spisak, Jongsoo Park, Joseph Rocca, Joshua Johnstun, Joshua Saxe, Junteng Jia, Kalyan Vasudevan Alwala, Karthik Prasad, Kartikeya Upasani, Kate Plawiak, Ke Li, Kenneth Heafield, Kevin Stone, Khalid El-Arini, Krithika Iyer, Kshitiz Malik, Kuenley Chiu, Kunal Bhalla, Kushal Lakhota, Lauren Rantala-Yeary, Laurens van der Maaten, Lawrence Chen, Liang Tan, Liz Jenkins, Louis Martin, Lovish Madaan, Lubo Malo, Lukas Blecher, Lukas Landzaat, Luke de Oliveira, Madeline Muzzi, Mahesh Pasupuleti, Mannat Singh, Manohar Paluri, Marcin Kardas, Maria Tsimpoukelli, Mathew Oldham, Mathieu Rita, Maya Pavlova, Melanie Kambadur, Mike Lewis, Min Si, Mitesh Kumar Singh, Mona Hassan, Naman Goyal, Narjes Torabi, Nikolay Bashlykov, Nikolay Bogoychev, Niladri Chatterji, Ning Zhang, Olivier Duchenne, Onur Çelebi, Patrick Alrassy, Pengchuan Zhang, Pengwei Li, Petar Vasic, Peter Weng, Prajjwal Bhargava, Pratik Dubal, Praveen Krishnan, Punit Singh Koura, Puxin Xu, Qing He, Qingxiao Dong, Ragavan Srinivasan, Raj Ganapathy, Ramon Calderer, Ricardo Silveira Cabral, Robert Stojnic, Roberta Raileanu, Rohan Maheswari, Rohit Girdhar, Rohit Patel, Romain Sauvestre, Ronnie Polidoro, Roshan Sumbaly, Ross Taylor, Ruan Silva, Rui Hou, Rui Wang, Saghar Hosseini, Sahana Chennabasappa, Sanjay Singh, Sean Bell, Seohyun Sonia Kim, Sergey Edunov, Shaoliang Nie, Sharan Narang, Sharath Raparthy, Sheng Shen, Shengye Wan, Shruti Bhosale, Shun Zhang, Simon Vandenbende, Soumya Batra, Spencer Whitman, Sten Sootla, Stephane Collot, Suchin Gururangan, Sydney Borodinsky, Tamar Herman, Tara Fowler, Tarek Sheasha, Thomas Georgiou, Thomas Scialom, Tobias Speckbacher, Todor Mihaylov, Tong Xiao, Ujjwal

Karn, Vedanuj Goswami, Vibhor Gupta, Vignesh Ramanathan, Viktor Kerkez, Vincent Gonquet, Virginie Do, Vish Vogeti, Vítor Albiero, Vladan Petrovic, Weiwei Chu, Wenhan Xiong, Wenyin Fu, Whitney Meers, Xavier Martinet, Xiaodong Wang, Xiaofang Wang, Xiaoqing Ellen Tan, Xide Xia, Xinfeng Xie, Xuchao Jia, Xuewei Wang, Yaelle Goldschlag, Yashesh Gaur, Yasmine Babaei, Yi Wen, Yiwen Song, Yuchen Zhang, Yue Li, Yuning Mao, Zacharie Delpierre Coudert, Zheng Yan, Zhengxing Chen, Zoe Papakipos, Aaditya Singh, Aayushi Srivastava, Abha Jain, Adam Kelsey, Adam Shajnfeld, Adithya Gangidi, Adolfo Victoria, Ahuva Goldstand, Ajay Menon, Ajay Sharma, Alex Boesenberg, Alexei Baevski, Allie Feinstein, Amanda Kallet, Amit Sangani, Amos Teo, Anam Yunus, Andrei Lupu, Andres Alvarado, Andrew Caples, Andrew Gu, Andrew Ho, Andrew Poulton, Andrew Ryan, Ankit Ramchandani, Annie Dong, Annie Franco, Anuj Goyal, Aparajita Saraf, Arkabandhu Chowdhury, Ashley Gabriel, Ashwin Bharambe, Assaf Eisenman, Azadeh Yazdan, Beau James, Ben Maurer, Benjamin Leonhardi, Bernie Huang, Beth Loyd, Beto De Paola, Bhargavi Paranjape, Bing Liu, Bo Wu, Boyu Ni, Braden Hancock, Bram Wasti, Brandon Spence, Brani Stojkovic, Brian Gamido, Britt Montalvo, Carl Parker, Carly Burton, Catalina Mejia, Ce Liu, Changhan Wang, Changkyu Kim, Chao Zhou, Chester Hu, Ching-Hsiang Chu, Chris Cai, Chris Tindal, Christoph Feichtenhofer, Cynthia Gao, Damon Civin, Dana Beaty, Daniel Kreymer, Daniel Li, David Adkins, David Xu, Davide Testuggine, Delia David, Devi Parikh, Diana Liskovich, Didem Foss, Dingkang Wang, Duc Le, Dustin Holland, Edward Dowling, Eissa Jamil, Elaine Montgomery, Eleonora Presani, Emily Hahn, Emily Wood, Eric-Tuan Le, Erik Brinkman, Esteban Arcaute, Evan Dunbar, Evan Smothers, Fei Sun, Felix Kreuk, Feng Tian, Filippos Kokkinos, Firat Ozgenel, Francesco Caggioni, Frank Kanayet, Frank Seide, Gabriela Medina Florez, Gabriella Schwarz, Gada Badeer, Georgia Swee, Gil Halpern, Grant Herman, Grigory Sizov, Guangyi, Zhang, Guna Lakshminarayanan, Hakan Inan, Hamid Shojanazeri, Han Zou, Hannah Wang, Hanwen Zha, Haroun Habeeb, Harrison Rudolph, Helen Suk, Henry Aspegren, Hunter Goldman, Hongyuan Zhan, Ibrahim Damlaj, Igor Molybog, Igor Tufanov, Ilias Leontiadis, Irina-Elena Veliche, Itai Gat, Jake Weissman, James Geboski, James Kohli, Janice Lam, Japhet Asher, Jean-Baptiste Gaya, Jeff Marcus, Jeff Tang, Jennifer Chan, Jenny Zhen, Jeremy Reizenstein, Jeremy Teboul, Jessica Zhong, Jian Jin, Jingyi Yang, Joe Cummings, Jon Carvill, Jon Shepard, Jonathan McPhie, Jonathan Torres, Josh Ginsburg, Junjie Wang, Kai Wu, Kam Hou U, Karan Saxena, Kartikay Khandelwal, Katayoun Zand, Kathy Matosich, Kaushik Veeraraghavan, Kelly Michelena, Keqian Li, Kiran Jagadeesh, Kun Huang, Kunal Chawla, Kyle Huang, Lailin Chen, Lakshya Garg, Lavender A, Leandro Silva, Lee Bell, Lei Zhang, Liangpeng Guo, Licheng Yu, Liron Moshkovich, Luca Wehrstedt, Madian Khabsa, Manav Avalani, Manish Bhatt, Martynas Mankus, Matan Hasson, Matthew Lennie, Matthias Reso, Maxim Groshev, Maxim Naumov, Maya Lathi, Meghan Keneally, Miao Liu, Michael L. Seltzer, Michal Valko, Michelle Restrepo, Mihir Patel, Mik Vyatskov, Mikayel Samvelyan, Mike Clark, Mike Macey, Mike Wang, Miquel Jubert Hermoso, Mo Metanat, Mohammad Rastegari, Munish Bansal, Nandhini Santhanam, Natascha Parks, Natasha White, Navyata Bawa, Nayan Singhal, Nick Egebo, Nicolas Usunier, Nikhil Mehta, Nikolay Pavlovich Laptev, Ning Dong, Norman Cheng, Oleg Chernoguz, Olivia Hart, Omkar Salpekar, Ozlem Kalinli, Parkin Kent, Parth Parekh, Paul Saab, Pavan Balaji, Pedro Rittner, Philip Bontrager, Pierre Roux, Piotr Dollar, Polina Zvyagina, Prashant Ratanchandani, Pritish Yuvraj, Qian Liang, Rachad Alao, Rachel Rodriguez, Rafi Ayub, Raghotham Murthy, Raghu Nayani, Rahul Mitra, Rangaprabhu Parthasarathy, Raymond Li, Rebekkah Hogan, Robin Battey, Rocky Wang, Russ Howes, Ruty Rinott, Sachin Mehta, Sachin Siby, Sai Jayesh Bondu, Samyak Datta, Sara Chugh, Sara Hunt, Sargun Dhillon, Sasha Sidorov, Satadru Pan, Saurabh

Mahajan, Saurabh Verma, Seiji Yamamoto, Sharadh Ramaswamy, Shaun Lindsay, Shaun Lindsay, Sheng Feng, Shenghao Lin, Shengxin Cindy Zha, Shishir Patil, Shiva Shankar, Shuqiang Zhang, Shuqiang Zhang, Sinong Wang, Sneha Agarwal, Soji Sajuyigbe, Soumith Chintala, Stephanie Max, Stephen Chen, Steve Kehoe, Steve Satterfield, Sudarshan Govindaprasad, Sumit Gupta, Summer Deng, Sungmin Cho, Sunny Virk, Suraj Subramanian, Sy Choudhury, Sydney Goldman, Tal Remez, Tamar Glaser, Tamara Best, Thilo Koehler, Thomas Robinson, Tianhe Li, Tianjun Zhang, Tim Matthews, Timothy Chou, Tzook Shaked, Varun Vontimitta, Victoria Ajayi, Victoria Montanez, Vijai Mohan, Vinay Satish Kumar, Vishal Mangla, Vlad Ionescu, Vlad Poenaru, Vlad Tiberiu Mihailescu, Vladimir Ivanov, Wei Li, Wencheng Wang, Wenwen Jiang, Wes Bouaziz, Will Constable, Xiaocheng Tang, Xiaojian Wu, Xiaolan Wang, Xilun Wu, Xinbo Gao, Yaniv Kleinman, Yanjun Chen, Ye Hu, Ye Jia, Ye Qi, Yenda Li, Yilin Zhang, Ying Zhang, Yossi Adi, Youngjin Nam, Yu, Wang, Yu Zhao, Yuchen Hao, Yundi Qian, Yunlu Li, Yuzi He, Zach Rait, Zachary DeVito, Zef Rosnbrick, Zhaoduo Wen, Zhenyu Yang, Zhiwei Zhao, and Zhiyu Ma. The llama 3 herd of models, 2024. URL <https://arxiv.org/abs/2407.21783>.

Edward J. Hu, Yelong Shen, Phillip Wallis, Zeyuan Allen-Zhu, Yuanzhi Li, Shean Wang, Lu Wang, and Weizhu Chen. Lora: Low-rank adaptation of large language models, 2021. URL <https://arxiv.org/abs/2106.09685>.

Drew A. Hudson and Christopher D. Manning. Gqa: A new dataset for real-world visual reasoning and compositional question answering, 2019.

Max Jaderberg, Volodymyr Mnih, Wojciech Marian Czarnecki, Tom Schaul, Joel Z Leibo, David Silver, and Koray Kavukcuoglu. Reinforcement learning with unsupervised auxiliary tasks. In *International Conference on Learning Representations*, 2017. URL <https://openreview.net/forum?id=SJ6yPD5xg>.

Siddharth Joshi, Besmira Nushi, Vidhisha Balachandran, Varun Chandrasekaran, Vibhav Vineet, Neel Joshi, and Baharan Mirzasoleiman. Mm-gen: Enhancing task performance through targeted multimodal data curation, 2025. URL <https://arxiv.org/abs/2501.04155>.

Ansh Khurana, Sujoy Paul, Piyush Rai, Soma Biswas, and Gaurav Aggarwal. Sita: Single image test-time adaptation, 2022. URL <https://arxiv.org/abs/2112.02355>.

Zhengfeng Lai, Haoping Bai, Haotian Zhang, Xianzhi Du, Jiulong Shan, Yinfeng Yang, Chen-Nee Chuah, and Meng Cao. Empowering unsupervised domain adaptation with large-scale pre-trained vision-language models. In *2024 IEEE/CVF Winter Conference on Applications of Computer Vision (WACV)*, pages 2679–2689, 2024. doi: 10.1109/WACV57701.2024.00267.

Alex Levenshtein, Alborz Rezazadeh Sereshkeh, and Konstantinos G. Derpanis. Datnet: Dense auxiliary tasks for object detection. *2020 IEEE Winter Conference on Applications of Computer Vision (WACV)*, pages 1408–1416, 2020. URL <https://api.semanticscholar.org/CorpusID:211733435>.

Junnan Li, Dongxu Li, Silvio Savarese, and Steven Hoi. Blip-2: Bootstrapping language-image pre-training with frozen image encoders and large language models, 2023. URL <https://arxiv.org/abs/2301.12597>.

- Haotian Liu, Chunyuan Li, Qingyang Wu, and Yong Jae Lee. Visual instruction tuning, 2023. URL <https://arxiv.org/abs/2304.08485>.
- Ilya Loshchilov and Frank Hutter. Decoupled weight decay regularization, 2019. URL <https://arxiv.org/abs/1711.05101>.
- Brandon McKinzie, Zhe Gan, Jean-Philippe Fauconnier, Sam Dodge, Bowen Zhang, Philipp Dufter, Dhruti Shah, Xianzhi Du, Futang Peng, Floris Weers, Anton Belyi, Haotian Zhang, Karanjeet Singh, Doug Kang, Ankur Jain, Hongyu Hè, Max Schwarzer, Tom Gunter, Xiang Kong, Aonan Zhang, Jianyu Wang, Chong Wang, Nan Du, Tao Lei, Sam Wiseman, Guoli Yin, Mark Lee, Zirui Wang, Ruoming Pang, Peter Grasch, Alexander Toshev, and Yinfei Yang. Mm1: Methods, analysis & insights from multimodal llm pre-training, 2024. URL <https://arxiv.org/abs/2403.09611>.
- Sewon Min, Xinxi Lyu, Ari Holtzman, Mikel Artetxe, Mike Lewis, Hannaneh Hajishirzi, and Luke Zettlemoyer. Rethinking the role of demonstrations: What makes in-context learning work? In Yoav Goldberg, Zornitsa Kozareva, and Yue Zhang, editors, *Proceedings of the 2022 Conference on Empirical Methods in Natural Language Processing*, pages 11048–11064, Abu Dhabi, United Arab Emirates, December 2022. Association for Computational Linguistics. doi: 10.18653/v1/2022.emnlp-main.759. URL <https://aclanthology.org/2022.emnlp-main.759>.
- Shervin Minaee, Tomas Mikolov, Narjes Nikzad, Meysam Chenaghlu, Richard Socher, Xavier Amatriain, and Jianfeng Gao. Large language models: A survey, 2025. URL <https://arxiv.org/abs/2402.06196>.
- Abhishek Narayanan, Rushabh Musthyala, Rahul Sankar, Anirudh Prasad Nistala, Pranav Singh, and Jacopo Cirrone. Free form medical visual question answering in radiology, 2024. URL <https://arxiv.org/abs/2401.13081>.
- Gustaw Opiełka, Hannes Rosenbusch, and Claire E. Stevenson. Analogical reasoning inside large language models: Concept vectors and the limits of abstraction, 2025. URL <https://arxiv.org/abs/2503.03666>.
- Ethan Perez, Saffron Huang, Francis Song, Trevor Cai, Roman Ring, John Aslanides, Amelia Glaese, Nat McAleese, and Geoffrey Irving. Red teaming language models with language models, 2022. URL <https://arxiv.org/abs/2202.03286>.
- Alec Radford, Jong Wook Kim, Chris Hallacy, Aditya Ramesh, Gabriel Goh, Sandhini Agarwal, Girish Sastry, Amanda Askell, Pamela Mishkin, Jack Clark, Gretchen Krueger, and Ilya Sutskever. Learning transferable visual models from natural language supervision, 2021. URL <https://arxiv.org/abs/2103.00020>.
- Jack W. Rae, Sebastian Borgeaud, Trevor Cai, Katie Millican, Jordan Hoffmann, Francis Song, John Aslanides, Sarah Henderson, Roman Ring, Susannah Young, Eliza Rutherford, Tom Hennigan, Jacob Menick, Albin Cassirer, Richard Powell, George van den Driessche, Lisa Anne Hendricks, Maribeth Rauh, Po-Sen Huang, Amelia Glaese, Johannes Welbl, Sumanth Dathathri, Saffron Huang, Jonathan Uesato, John Mellor, Irina Higgins, Antonia Creswell, Nat McAleese, Amy Wu, Erich Elsen, Siddhant Jayakumar, Elena Buchatskaya, David Budden, Esme Sutherland, Karen

Simonyan, Michela Paganini, Laurent Sifre, Lena Martens, Xiang Lorraine Li, Adhiguna Kuncoro, Aida Nematzadeh, Elena Gribovskaya, Domenic Donato, Angeliki Lazaridou, Arthur Mensch, Jean-Baptiste Lespiau, Maria Tsimpoukelli, Nikolai Grigorev, Doug Fritz, Thibault Sottiaux, Mantas Pajarskas, Toby Pohlen, Zhitao Gong, Daniel Toyama, Cyprien de Masson d’Autume, Yujia Li, Tayfun Terzi, Vladimir Mikulik, Igor Babuschkin, Aidan Clark, Diego de Las Casas, Aurelia Guy, Chris Jones, James Bradbury, Matthew Johnson, Blake Hechtman, Laura Weidinger, Iason Gabriel, William Isaac, Ed Lockhart, Simon Osindero, Laura Rimell, Chris Dyer, Oriol Vinyals, Kareem Ayoub, Jeff Stanway, Lorrayne Bennett, Demis Hassabis, Koray Kavukcuoglu, and Geoffrey Irving. Scaling language models: Methods, analysis & insights from training gopher, 2022. URL <https://arxiv.org/abs/2112.11446>.

Banafsheh Rafiee, Sina Ghiassian, Jun Jin, Richard Sutton, Jun Luo, and Adam White. Auxiliary task discovery through generate-and-test. In Sarath Chandar, Razvan Pascanu, Hanie Sedghi, and Doina Precup, editors, *Proceedings of The 2nd Conference on Lifelong Learning Agents*, volume 232 of *Proceedings of Machine Learning Research*, pages 703–714. PMLR, 22–25 Aug 2023. URL <https://proceedings.mlr.press/v232/rafiee23a.html>.

Laura Ruis, Maximilian Mozes, Juhan Bae, Siddhartha Rao Kamalakara, Dwarak Talupuru, Acyr Locatelli, Robert Kirk, Tim Rocktäschel, Edward Grefenstette, and Max Bartolo. Procedural knowledge in pretraining drives reasoning in large language models, 2025. URL <https://arxiv.org/abs/2411.12580>.

Mikayel Samvelyan, Sharath Chandra Raparthy, Andrei Lupu, Eric Hambro, Aram H. Markosyan, Manish Bhatt, Yuning Mao, Minqi Jiang, Jack Parker-Holder, Jakob Foerster, Tim Rocktäschel, and Roberta Raileanu. Rainbow teaming: Open-ended generation of diverse adversarial prompts, 2024. URL <https://arxiv.org/abs/2402.16822>.

Baifeng Shi, Judy Hoffman, Kate Saenko, Trevor Darrell, and Huijuan Xu. Auxiliary task reweighting for minimum-data learning. In *Proceedings of the 34th International Conference on Neural Information Processing Systems*, NIPS ’20, Red Hook, NY, USA, 2020. Curran Associates Inc. ISBN 9781713829546.

Yu Sun, Eric Tzeng, Trevor Darrell, and Alexei A. Efros. Unsupervised domain adaptation through self-supervision, 2019a. URL <https://arxiv.org/abs/1909.11825>.

Yu Sun, Xiaolong Wang, Zhuang Liu, John Miller, Alexei A. Efros, and Moritz Hardt. Test-time training for out-of-distribution generalization. *CoRR*, abs/1909.13231, 2019b. URL <https://arxiv.org/abs/1909.13231>.

Gemma Team, Aishwarya Kamath, Johan Ferret, Shreya Pathak, Nino Vieillard, Ramona Merhej, Sarah Perrin, Tatiana Matejovicova, Alexandre Ramé, Morgane Rivière, Louis Rouillard, Thomas Mesnard, Geoffrey Cideron, Jean bastien Grill, Sabela Ramos, Edouard Yvinec, Michelle Casbon, Etienne Pot, Ivo Penchev, Gaël Liu, Francesco Visin, Kathleen Kenealy, Lucas Beyer, Xiaohai Zhai, Anton Tsitsulin, Robert Busa-Fekete, Alex Feng, Noveen Sachdeva, Benjamin Coleman, Yi Gao, Basil Mustafa, Iain Barr, Emilio Parisotto, David Tian, Matan Eyal, Colin Cherry, Jan-Thorsten Peter, Danila Sinopalnikov, Surya Bhupatiraju, Rishabh Agarwal, Mehran Kazemi, Dan Malkin, Ravin Kumar, David Vilar, Idan Brusilovsky, Jiaming Luo, Andreas Steiner, Abe Friesen, Abhanshu Sharma, Abheesht Sharma, Adi Mayrav Gilady, Adrian Goedeckemeyer, Alaa

Saade, Alex Feng, Alexander Kolesnikov, Alexei Bendebury, Alvin Abdagic, Amit Vadi, András György, André Susano Pinto, Anil Das, Ankur Bapna, Antoine Miech, Antoine Yang, Antonia Paterson, Ashish Shenoy, Ayan Chakrabarti, Bilal Piot, Bo Wu, Bobak Shahriari, Bryce Petrini, Charlie Chen, Charline Le Lan, Christopher A. Choquette-Choo, CJ Carey, Cormac Brick, Daniel Deutsch, Danielle Eisenbud, Dee Cattle, Derek Cheng, Dimitris Paparas, Divyashree Shivakumar Sreepathihalli, Doug Reid, Dustin Tran, Dustin Zelle, Eric Noland, Erwin Huizenga, Eugene Kharitonov, Frederick Liu, Gagik Amirkhanyan, Glenn Cameron, Hadi Hashemi, Hanna Klimczak-Plucińska, Harman Singh, Harsh Mehta, Harshal Tushar Lehri, Hussein Hazimeh, Ian Ballantyne, Idan Szpektor, Ivan Nardini, Jean Pouget-Abadie, Jetha Chan, Joe Stanton, John Wieting, Jonathan Lai, Jordi Orbay, Joseph Fernandez, Josh Newlan, Ju yeong Ji, Jyotinder Singh, Kat Black, Kathy Yu, Kevin Hui, Kiran Vodrahalli, Klaus Greff, Linhai Qiu, Marcella Valentine, Marina Coelho, Marvin Ritter, Matt Hoffman, Matthew Watson, Mayank Chaturvedi, Michael Moynihan, Min Ma, Nabila Babar, Natasha Noy, Nathan Byrd, Nick Roy, Nikola Momchev, Nilay Chauhan, Noveen Sachdeva, Oskar Bunyan, Pankil Botarda, Paul Caron, Paul Kishan Rubenstein, Phil Culliton, Philipp Schmid, Pier Giuseppe Sessa, Pingmei Xu, Piotr Stanczyk, Pouya Tafti, Rakesh Shivanna, Renjie Wu, Renke Pan, Reza Rokni, Rob Willoughby, Rohith Vallu, Ryan Mullins, Sammy Jerome, Sara Smoot, Sertan Girgin, Shariq Iqbal, Shashir Reddy, Shruti Sheth, Siim Põder, Sijal Bhatnagar, Sindhu Raghuram Panyam, Sivan Eiger, Susan Zhang, Tianqi Liu, Trevor Yacovone, Tyler Liechty, Uday Kalra, Utku Evcı, Vedant Misra, Vincent Roseberry, Vlad Feinberg, Vlad Kolesnikov, Woohyun Han, Woosuk Kwon, Xi Chen, Yinlam Chow, Yuvein Zhu, Zichuan Wei, Zoltan Egyed, Victor Cotruta, Minh Giang, Phoebe Kirk, Anand Rao, Kat Black, Nabila Babar, Jessica Lo, Erica Moreira, Luiz Gustavo Martins, Omar Sanseviero, Lucas Gonzalez, Zach Gleicher, Tris Warkentin, Vahab Mirrokni, Evan Senter, Eli Collins, Joelle Barral, Zoubin Ghahramani, Raia Hadsell, Yossi Matias, D. Sculley, Slav Petrov, Noah Fiedel, Noam Shazeer, Oriol Vinyals, Jeff Dean, Demis Hassabis, Koray Kavukcuoglu, Clement Farabet, Elena Buchatskaya, Jean-Baptiste Alayrac, Rohan Anil, Dmitry Lepikhin, Sebastian Borgeaud, Olivier Bachem, Armand Joulin, Alek Andreev, Cassidy Hardin, Robert Dadashi, and Léonard Hussenot. Gemma 3 technical report, 2025. URL <https://arxiv.org/abs/2503.19786>.

Hugo Touvron, Louis Martin, Kevin Stone, Peter Albert, Amjad Almahairi, Yasmine Babaei, Nikolay Bashlykov, Soumya Batra, Prajjwal Bhargava, Shruti Bhosale, Dan Bikel, Lukas Blecher, Cristian Canton Ferrer, Moya Chen, Guillem Cucurull, David Esiobu, Jude Fernandes, Jeremy Fu, Wenyin Fu, Brian Fuller, Cynthia Gao, Vedanuj Goswami, Naman Goyal, Anthony Hartshorn, Saghar Hosseini, Rui Hou, Hakan Inan, Marcin Kardas, Viktor Kerkez, Madian Khabsa, Isabel Kloumann, Artem Korenev, Punit Singh Koura, Marie-Anne Lachaux, Thibaut Lavril, Jenya Lee, Diana Liskovich, Yinghai Lu, Yuning Mao, Xavier Martinet, Todor Mihaylov, Pushkar Mishra, Igor Molybog, Yixin Nie, Andrew Poulton, Jeremy Reizenstein, Rashi Rungta, Kalyan Saladi, Alan Schelten, Ruan Silva, Eric Michael Smith, Ranjan Subramanian, Xiaoqing Ellen Tan, Binh Tang, Ross Taylor, Adina Williams, Jian Xiang Kuan, Puxin Xu, Zheng Yan, Iliyan Zarov, Yuchen Zhang, Angela Fan, Melanie Kambadur, Sharan Narang, Aurelien Rodriguez, Robert Stojnic, Sergey Edunov, and Thomas Scialom. Llama 2: Open foundation and fine-tuned chat models, 2023. URL <https://arxiv.org/abs/2307.09288>.

Dequan Wang, Evan Shelhamer, Shaoteng Liu, Bruno Olshausen, and Trevor Darrell. Tent: Fully test-time adaptation by entropy minimization. In *International Conference on Learning Representations*, 2021. URL <https://openreview.net/forum?id=uXl3bZLkr3c>.

- Weiyun Wang, Zhe Chen, Wenhui Wang, Yue Cao, Yangzhou Liu, Zhangwei Gao, Jinguo Zhu, Xizhou Zhu, Lewei Lu, Yu Qiao, and Jifeng Dai. Enhancing the reasoning ability of multimodal large language models via mixed preference optimization, 2024. URL <https://arxiv.org/abs/2411.10442>.
- Zhiqing Xiao, Haobo Wang, Ying Jin, Lei Feng, Gang Chen, Fei Huang, and Junbo Zhao. SPA: A graph spectral alignment perspective for domain adaptation. In *Thirty-seventh Conference on Neural Information Processing Systems*, 2023. URL <https://openreview.net/forum?id=lp9LZPVtZ>.
- Shaoan Xie, Zibin Zheng, Liang Chen, and Chuan Chen. Learning semantic representations for unsupervised domain adaptation. In Jennifer Dy and Andreas Krause, editors, *Proceedings of the 35th International Conference on Machine Learning*, volume 80 of *Proceedings of Machine Learning Research*, pages 5423–5432. PMLR, 10–15 Jul 2018. URL <https://proceedings.mlr.press/v80/xie18c.html>.
- Xiang Yue, Yuansheng Ni, Kai Zhang, Tianyu Zheng, Ruoqi Liu, Ge Zhang, Samuel Stevens, Dongfu Jiang, Weiming Ren, Yuxuan Sun, Cong Wei, Botao Yu, Ruibin Yuan, Renliang Sun, Ming Yin, Boyuan Zheng, Zhenzhu Yang, Yibo Liu, Wenhao Huang, Huan Sun, Yu Su, and Wenhui Chen. Mmmu: A massive multi-discipline multimodal understanding and reasoning benchmark for expert agi, 2024. URL <https://arxiv.org/abs/2311.16502>.
- Yuxiang Zhai, Shengbang Tong, Xiao Li, Mu Cai, Qing Qu, Yong Jae Lee, and Yi Ma. Investigating the catastrophic forgetting in multimodal large language model fine-tuning. In *Conference on Parsimony and Learning (Proceedings Track)*, 2023. URL <https://openreview.net/forum?id=g7rMSiNtmA>.
- Sheng Zhang, Yanbo Xu, Naoto Usuyama, Hanwen Xu, Jaspreet Bagga, Robert Tinn, Sam Preston, Rajesh Rao, Mu Wei, Naveen Valluri, Cliff Wong, Andrea Tupini, Yu Wang, Matt Mazzola, Swadheen Shukla, Lars Liden, Jianfeng Gao, Matthew P. Lungren, Tristan Naumann, Sheng Wang, and Hoifung Poon. Biomedclip: a multimodal biomedical foundation model pretrained from fifteen million scientific image-text pairs, 2024. URL <https://arxiv.org/abs/2303.00915>.
- Siyan Zhao, Tung Nguyen, and Aditya Grover. Probing the decision boundaries of in-context learning in large language models. In *ICML 2024 Workshop on In-Context Learning*, 2024. URL <https://openreview.net/forum?id=rfCtCcPuSt>.
- Thomas P. Zollo, Nikita Rajaneesh, Richard Zemel, Talia B. Gillis, and Emily Black. Towards effective discrimination testing for generative ai, 2024. URL <https://arxiv.org/abs/2412.21052>.
- Yang Zou, Zhiding Yu, B. V. K. Vijaya Kumar, and Jinsong Wang. Domain adaptation for semantic segmentation via class-balanced self-training, 2018. URL <https://arxiv.org/abs/1810.07911>.



Q: Where is the abnormality?
Ours: rib cage
Base MLLM: right lung

What is unusual or unique about this image?

This x-ray image is considered unusual or unique because it shows the ribs and the heart on the left side of the image, when it should be on the right. This can be indicative of a congenital heart defect called dextrocardia. However, this is not the only reason this image would be unusual or unique. The clavicles are in a partially inverted position. The clavicle on the right is visible on the left side of the image, and the clavicle on the left is visible on the right side of the image.

What details might someone easily overlook?

The image is a chest x-ray that appears to show a heart of normal size and shape, but upon closer inspection, there is a subtle indication of an enlarged heart. The heart is not clearly enlarged, but it is slightly larger than normal based on the ribs and lung contours. The lungs appear as dark gray shapes with visible air-filled pockets, which are typical of a normal chest x-ray. The bones of the rib cage are also visible, providing a framework for the lungs and heart. The most notable feature of this image is the slight enlargement of the heart, which can be seen as a subtle bulge in the midline of

Figure 6: In this example from VQA-Rad, where the warmed-up MLLM responds incorrectly while the base model answers correctly. Both of these auxiliary task outputs contain hallucinations about the ribs, heart and clavicle which likely led to the model answering incorrectly.

Appendix A. Additional Experiment Details and Results

Here, we discuss failure modes of our method and include more experiment details. Our code is available at <https://github.com/nrajanee/test-time-warmup-mllms>.

A.1. Failure modes of our method

By generating the auxiliary warm-up data with the target MLLM, we remove the need for labeled datasets, though this introduces a key failure mode. The MLLM may hallucinate, and although CLIP supervises these generations to curb hallucinations, subtle errors can evade detection. If CLIP selects such a hallucinated output, the ensuing answer may also be incorrect.

In Figures 6, 7 and 8 we show examples of this failure mode in MMMU, GQA and VQA-Rad.

A.2. Evaluation

Metric We evaluate models using zero-shot accuracy. For GQA, VQA-Rad, and VQAv2, a response is considered correct if it contains the ground-truth answer. Additionally, for VQAv2, which includes multiple annotations, we apply the standard soft-scoring scheme that assigns higher weight to answers occurring more frequently in the annotation set. For MMMU, we report accuracy using the official evaluation code Yue et al. (2024) 1. To ensure consistency, all baselines, methods



Q: Is the black and white picture both colorful and grassy?

Ours: yes, the picture is both colorful and grassy.

Base MLLM: no, the image is not both colorful and grassy.

What is unusual or unique about this image?

The image is unusual because a zebra is depicted in a mostly black and white tone, but the grasses surrounding the zebra are in color, which is not typical of this type of image.

Are there any signs, symbols, or text in this image? If so, what do they say?

The image is monochrome, and only contains a zebra. It does not include any signs, symbols, or text.

What does the background reveal about this image?

The background reveals that this image might be of a wild animal in its natural habitat. The image is in grayscale and the zebra appears to be standing in a field of grass that is dry.

Figure 7: In this GQA example, the warmed-up MLLM responds incorrectly while the base model answers correctly. Despite weighting all auxiliary task outputs equally and reshuffling them before each epoch, a single hallucinated output describing colorful grass, in contrast to the others’ grayscale description, still steers the model to the wrong answer.

and ablations use the same evaluation strategies for each dataset. The exact prompts and sampling parameters are provided in the appendix.

GQA, VQA-Rad, VQAV2 For evaluating Llama-3.2-11B-Vision-Instruct on these datasets we use the prompts shown in Table 3. To generate the responses from the model, we use greedy sampling and we set the sampling parameter `max_new_tokens = 128`.

MMMU For evaluating LLama-vision-instruct on MMMU we use the prompts shown in Table 3. To generate the responses from the model, we set the sampling parameters `max_new_tokens = 512`, `top_k = 50`, `top_p = 0.8`.

ICL + our auxiliary data The prompt for in context learning is shown in Table 3. For generating answers to questions, this prompt is prepended to the appropriate evaluation prompt.

A.3. Auxiliary data generation

For auxiliary task data generation we use the prompts shown in Table 3. We set temperature to 0.75 and all other sampling parameters are set to the default in huggingface.



Q: <image 1> The work in the image shows the influence of Western art in its use of
 (A) classical contrapposto
 (B) atmospheric perspective
 (C) Di sotto in su
 (D) tenebrism

Ours: The work in the image shows the influence of Western art in its use of classical contrapposto, which is a pose where the weight-bearing leg is relaxed and the free leg is tense, creating a sense of movement and balance. This technique was popularized by ancient Greek and Roman artists and has been adopted by many artists throughout history, including those in the Renaissance period.

Answer: (A)

Base MLLM: The image depicts a painting of a man and a woman in a forest, with the man holding a bow and arrow. The woman is lying on the ground, and there are trees and foliage surrounding them. The painting is done in a style that is reminiscent of Western art, with the use of chiaroscuro and the depiction of the human form in a realistic manner.

The correct answer is (B) atmospheric perspective.

What actions are the subjects performing in this image?

The subject in the center of the image is depicted in a dynamic pose, seemingly poised for action. The surrounding text, which appears to be in Persian, provides context for the scene but does not directly describe the actions. Based on the attire and the environment, it is likely that the subject is a prince or a high-ranking figure, possibly engaged in a hunting or military expedition. The bow and arrow held by the subject suggest a readiness for combat or the pursuit of prey, indicating that the action is either related to hunting or a form of military engagement. Without a detailed description of the text, the exact nature of the action cannot be definitively determined.

Explain the possible relationships or roles of the people, animals, or objects in this scene. What hints or clues suggest these relationships?

The image depicts a scene from a folio of the Shahnameh, the national epic of Persia, written by the Persian poet Ferdowsi between 977 and 1010. The scene is set in a forest and features a hunter, likely Rostam, the protagonist of the Shahnameh, on horseback with his bow and arrows. The hunter is shown in the act of shooting an arrow at a deer, which is running away from him. There are other animals in the background, including a wolf and a bear. The hunter is dressed in traditional Persian attire, consisting of a tunic, pants, and a turban.

Figure 8: In this MMMU example, the warmed-up MLLM responds incorrectly while the base model answers correctly. Both of these auxiliary task outputs emphasized the pose and action of the figure rather than the scenery, which likely led the model to answer incorrectly.

Table 3: Prompt templates for evaluation and auxiliary data generation. The sample model input provides a specific example input given to a model (chat tags are excluded). In the evaluation prompt we replace question with image specific question. In the auxiliary task data generation prompt we provide each of the task prompts listed in Figure 2. For in context learning, we concatenate the auxiliary task responses and provide it in context to the model. In addition to all these prompts the image is passed to the model for generation.

Prompt objective: Evaluate a model on GQA, VQAV2, VQA-Rad

Prompt template: {question} Answer the question using a single word or phrase.

Sample model input: What is behind the white bench? Answer the question using a single word or phrase

Prompt objective: Evaluate a model on MMMU

Prompt template: {question}

Answer the question above by strictly following the guidelines below. Your main goal is to provide the correct answer in the response. Do not deviate from the guidelines below.

1. Be Concise - Provide a single word or brief phrase for the answer whenever possible, adhering to the final answer format.
2. Multiple-Choice (A, B, C, D) - Respond only with the correct letter in square brackets, for example, [A].
3. If Reasoning is Needed - Do not end your response with reasoning alone; always include the final answer as specified below.
4. Final Answer Format - The correct answer must appear on the last line, preceded by the text: "Correct answer:" - The answer should be either a single word/phrase or a letter in square brackets (e.g., [A]). - If unsure, provide your best logical guess.

Sample model input: Margaret Gere's [image 1] was made in which medium? (A) Egg tempera
(B) Watercolour (C) Ink (D) Oil paint

Answer the question above by strictly following the guidelines below... (same rules as above).

Prompt objective: Generate auxiliary task data

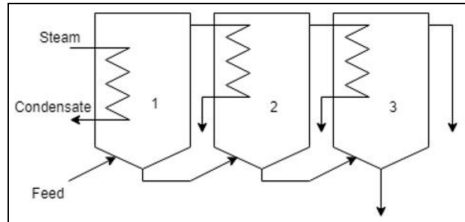
Prompt template: {Auxiliary task prompt}

Sample model input: What objects or people are visible in this image?

Prompt objective: In context learning with our auxiliary data

Prompt template: Here are a detailed list of captions of the image: {concatenated_captions}. Answer the following question using these captions.

Sample model input: Here are a detailed list of captions of the image: The image shows a suitcase, mask and table. This image has a table placed in front of suitcase... Answer the following question using these captions.



What is happening in this image?

The image depicts a triple-effect evaporator, which is a type of evaporator that utilizes the heat from the vapor produced in one effect to drive the evaporation process in subsequent effects. This process allows for more efficient use of energy and can result in higher overall efficiency compared to single-effect evaporators.
In this diagram, the feed enters the first effect (1) and is heated by steam, causing some of the water to vaporize. The vapor produced in the first effect is then used as the heating medium for the second effect (2), where more water vaporizes. Similarly, the vapor from the second effect is used to heat the third effect (3).

Question: Q: What is the capacity of the forward feed evaporator shown in <image 1> in the provided setup?

- (A) $E_1 + E_2 + E_3$
- (B) E_3
- (C) E_1
- (D) $E_1 + E_2$

Ours:

Step 1: Understand the problem The problem presents a forward feed evaporator setup, which is a type of evaporator where the feed enters at one end and flows through each stage in sequence. The capacity of an evaporator refers to the amount of vapor produced per unit time.

Step 2: Identify the relevant information From the diagram, we can see that there are three stages (1, 2, and 3) in the evaporator. The feed enters at stage 1 and flows through each stage in sequence.

Step 3: Analyze the options Option (A) suggests that the capacity is the sum of the capacities of all three stages ($E_1 + E_2 + E_3$). Option (B) suggests that the capacity is only E_3 , which is the last stage. Option (C) suggests that the capacity is only E_1 , which is the first stage. Option (D) suggests that the capacity is the sum of the capacities of the first two stages ($E_1 + E_2$).

Step 4: Reasoning In a forward feed evaporator, the feed flows through each stage in sequence, and the vapor produced in each stage is collected and used as the feed for the next stage. Therefore, the capacity of the evaporator is the sum of the capacities of all three stages ($E_1 + E_2 + E_3$).

Answer (A)

Base MLLM:

Step 1: Understand the question

The question asks for the capacity of a forward feed evaporator in the provided setup.

Step 2: Identify the components

The setup consists of three evaporators (E_1 , E_2 , and E_3) with steam as the heating medium and condensate as the cooling medium.

Step 3: Analyze the flow

In a forward feed evaporator, the feed enters the first stage (E_1), and the vapor from each stage is used to heat the next stage. The condensate from each stage is removed and used as the cooling medium for the next stage.

Step 4: Determine the capacity

The capacity of an evaporator is determined by the amount of feed that can be processed per unit time. In this case, the capacity is limited by the first stage (E_1), as it is the only stage that receives fresh feed.

Step 5: Conclusion

Based on the analysis, the capacity of the forward feed evaporator is equal to the capacity of the first stage (E_1).

Answer (C)

Figure 9: Example in MMMU of where our "warmed up" MLLM answers correctly while the base MLLM fails. On the left we show the auxiliary prompt response that was the most relevant to the question and potentially aided the model for better reasoning. On the right, we show the answer response with correct reasoning highlighted in red for incorrect reasoning. Here the auxiliary response explicitly provides information relevant to the question, which demonstrates how these auxiliary task prompts can help the model focus²⁷ on the critical details needed to reach the right conclusion. TZ: this figure is very hard to see/readNR: done

